

# Long time stress relaxation of filled amorphous networks under uniaxial tension: dynamic constrained junction model

H. Konyali<sup>1,2</sup>, Y. Menceloglu<sup>1</sup> and B. Erman<sup>\*3</sup>

The dynamic constrained junction model, based on the equilibrium theory of rubber elasticity, is applied to study the effects of fillers on the relaxation of stress in uniaxially deformed rubbers. Only low degrees of reinforcement are considered where complications such as filler–filler interactions are not pronounced. The proposed model is based on a purely molecular picture of the network and attempts to explain the molecular origins of the deformation and time dependence of stress in filled rubbers. Comparison with experimental data on filled (poly)isoprene networks showed that the deformation and time dependence of lightly filled samples can be predicted satisfactorily by the model.

**Keywords:** Molecular theory of rubbers, Viscoelasticity, Constraints, Stress relaxation

## Introduction

When an amorphous polymeric network is stretched to a fixed length and kept at that length for a sufficiently long time, the force required to keep it at this length decreases until a finite value which is referred to as the force at equilibrium. Uniaxial data are generally presented in terms of the reduced stress,  $[f^*] = f/A_0(\lambda - \lambda^{-2})$ , where  $f$  is the force acting on the network,  $A_0$  is the undeformed cross-sectional area, and  $\lambda$  is the extension ratio defined as the ratio of the final length to the original length of the sample. In uniaxial tension, the phenomenological Mooney–Rivlin equation has been used to describe the force extension relation over a wide range of deformation<sup>1</sup>

$$[f^*] = 2C_1 + \frac{2C_2}{\lambda} \quad (1)$$

where,  $2C_1$  and  $2C_2$  are the phenomenological coefficients. Equation (1) serves as a good approximation both in equilibrium and out of equilibrium behaviour of networks. In the graph of reduced stress versus the reciprocal of extension ratio, referred to as the Mooney–Rivlin plot,  $2C_1$  and  $2C_2$  represent the intercept and the slope of the line respectively. In molecular interpretations of rubber elasticity, the  $2C_1$  intercept, known as the phantom network modulus, is associated with contributions from the network cycle rank proportional to the number of chains constituting the network, and the slope  $2C_2$  is associated with contributions from

constraints that affect the fluctuations of chains and junction points. Thus, the  $2C_1$  term reflects contributions from network topology, whereas the  $2C_2$  effect arises from effects of constraints that suppress the fluctuations in the system.<sup>2–6</sup> Theoretical considerations and neutron scattering experiments<sup>7–9</sup> show that fluctuations of junctions in amorphous unfilled networks are significant, being of the order of chain dimensions. Therefore, the contribution of fluctuations to stress is expected to be of major importance, both in equilibrium and out of equilibrium states and for unfilled and filled networks.

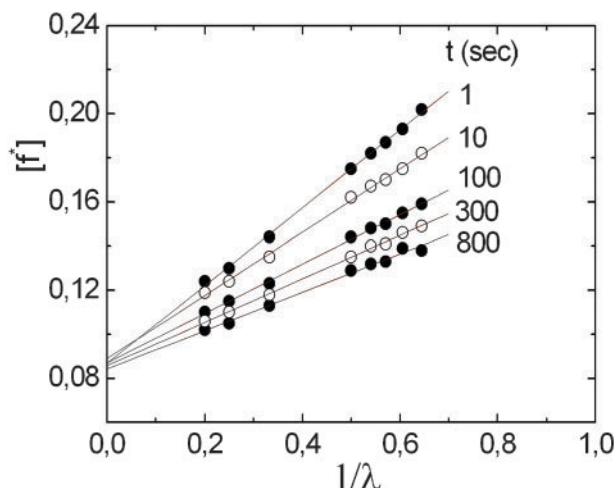
The long time relaxation experiments of Ferry *et al.*,<sup>10</sup> on lightly cross-linked unfilled polybutadiene networks showed that the time dependent Mooney–Rivlin equation describes the long time relaxation of uniaxial stress as well, with the observation that  $2C_1$  relaxes fast and is approximately independent from  $2C_2(t)$  which relaxes at a slower time scale. Thus, equation (1) serves as a good approximation both in equilibrium and out of equilibrium behaviour of networks. In Fig. 1, the long time relaxation results are presented in Mooney–Rivlin form for (poly)isoprene networks from the work of Konyali *et al.*<sup>11</sup> The slow relaxation of  $2C_2(t)$ , in line with its statistical mechanical interpretation, is an indication that the fluctuations in the system relax to an equilibrium value. Based on this view of time dependence of fluctuations, the authors recently proposed the dynamic constrained junction model for explaining the long time relaxation of stress in uniaxially stretched unfilled networks.<sup>11</sup> Comparison with results of (poly)isoprene networks showed good agreement with the predictions of the model. According to the equilibrium constrained junction model, the contributions to the reduced stress in excess of the  $2C_1$  value result from the energy stored upon deformation of the elastic constraints operating on the junctions. Thus, the model

<sup>1</sup>Faculty of Engineering and Natural Sciences, Sabanci University, Tuzla 34956, Istanbul, Turkey

<sup>2</sup>Tekno Kauçuk, GOSB, İhsan dede cad. Gebze 41480 Kocaeli, Turkey

<sup>3</sup>Department of Chemical and Biological Engineering, Koc University, Rumelifeneri Yolu, Sariyer 34450, Istanbul, Turkey

\*Corresponding author, email berman@ku.edu.tr



1 Isochronous Mooney–Rivlin plots for unfilled (poly)isoprene networks

introduces spring-like mechanisms that contribute to stress in addition to those from the network chains. If the network is stretched suddenly, the junctions behave as if they are securely embedded in their surroundings and their fluctuations are suppressed. This results in an affine-like transformation of the junctions. As time progresses, the junctions get a chance to diffuse to larger domains, and at equilibrium they reach their maximum fluctuations as obtained in the equilibrium case. As will be described in more detail in the section on ‘Theory and the model’, the only adjustable parameter of the model is the time dependent constraint parameter,  $\kappa(t)$ , that is inversely proportional to the size of the domain in which junctions fluctuate. At zero time, this domain is small and  $\kappa(t)$  is large, and vice versa for long times.

In the present paper, the authors apply the dynamic constrained junction model to study the effects of fillers on the time dependent properties of rubbers. The specific aim of the paper is to obtain a constitutive equation that describes the time dependent behaviour of filled rubbers. At this stage, the authors consider only low degrees of reinforcement where complications such as filler–filler interactions are not pronounced. Specifically, we keep the effective volume fraction of fillers below 0.12. Above this value, experiments that the authors performed but not reported show deviations from the simple additivity assumption that the authors propose by equation (18) given below. As is documented clearly in recent experiments,<sup>12</sup> interactions such as filler deformation and filler destruction are responsible for several microscopic phenomena that cannot be described in terms of the simple statistical theory of rubber elasticity on which the constrained junction model is based.<sup>7</sup> There are several excellent papers on the constitutive equations of filled rubbers.<sup>13–16</sup> In contrast to these highly successful theories, the dynamic constrained junction model is based on a purely molecular picture of the network and attempts to explain the molecular origins of the deformation and time dependence of stress in filled rubbers.

## Theory and the model

### Dynamic constrained junction model for unfilled networks

In a recent paper, the authors introduced the dynamic constrained junction model and showed that this model

explains stress relaxation of unfilled cross-linked (poly)isoprene successfully for different cross-link densities.<sup>11</sup>

In the equilibrium constrained junction model, the total force acting on the network is given as

$$f(t) = f_{ph} + f_{c,eq} \tag{2}$$

where,  $f_{ph}$  is the component of the force due to the phantom network, and  $f_{c,eq}$  is the equilibrium force due to the constraints.

At equilibrium, a network junction exhibits large scale fluctuations about its mean position resulting from large scale diffusive motions about their equilibrium configurations. According to the constrained junction model<sup>4–6</sup> a junction of the phantom network fluctuates in a domain of size  $\langle \Delta R^2 \rangle_{eq}^{1/2}$  where the subscript eq indicates that the system is at equilibrium. In the real network, due to entanglements, the junction is assumed to fluctuate in a smaller region of size  $\langle \Delta s^2 \rangle_{eq}^{1/2}$ . The deviation of a real network from the phantom network model is given by the constraint parameter,  $\kappa_{eq}$  defined as the ratio

$$\kappa_{eq} = \frac{\langle \Delta R^2 \rangle_{eq}}{\langle \Delta s^2 \rangle_{eq}} \tag{3}$$

The value of  $\kappa_{eq}$  varies between 0 for highly cross-linked networks and about 10 or 12 for lightly cross-linked networks.

In the dynamic constrained junction model, there is a third component of the force  $f_c(t)$  which relaxes to zero as time progresses. The total forces acting on the network for the dynamic constrained junction model is then

$$f(t) = f_{ph} + f_{c,eq} + f_c(t) \tag{4}$$

In this model  $f_c(t)$  depends on  $\kappa(t)$  which is the only additional parameter. In the literature, relaxations in networks are expressed either by a power law dependence of parameters on time or by a stretched exponent form. For relaxations in unfilled networks, the authors observed that the stretched exponent form of  $\kappa(t)$  is more satisfactory,<sup>11</sup> which the authors also adopt here

$$\kappa(t) = \kappa_0 \exp \left[ - \left( \frac{t}{\tau} \right)^\beta \right] \tag{5}$$

here,  $\tau$  is the characteristic time of relaxation of constraint effects,  $\beta$  is the exponent, and  $\kappa_0$  is the front factor.

For uniaxial deformation, the force on the phantom network is given as<sup>7</sup>

$$f_{ph} = \left( \frac{\xi kT}{L_0} \right) \left( \lambda - \frac{1}{\lambda^2} \right) \tag{6}$$

here,  $L_0$  is the length of sample, and  $\xi$  is the cycle rank of the network denoting the number of chains that should be cut in order to reduce the network to a tree. The second term  $f_{c,eq}$  in equation (4) is given by the constrained junction model as

$$f_{c,eq} = f_{ph} \left[ \frac{\lambda K(\lambda) - \lambda^{-2} K(\lambda^{-1})}{\lambda - \lambda^{-2}} \right] \tag{7}$$

where,

$$K(\lambda) = B \left[ \frac{\dot{B}}{B+1} + \kappa_{eq}^{-1} \frac{\lambda^2 \dot{B} + B}{B + \kappa_{eq} \lambda^{-2}} \right] \tag{8}$$

$$B = \kappa_{\text{eq}}^2 \frac{\lambda^2 - 1}{(\lambda^2 + \kappa_{\text{eq}})^2} \quad (9)$$

$$\dot{B} = B \left[ \frac{1}{\lambda^2 - 1} - \frac{2}{\lambda^2 + \kappa_{\text{eq}}} \right] \quad (10)$$

For small deviations from equilibrium the local entropy is assumed to exhibit dependence on parameters that are identical to the dependence in equilibrium.<sup>17</sup> This assumption allows us to extend the equilibrium constraint theory to the time domain, according to which the term  $f_c(t)$  in equation (4) now reads as

$$f_c(t) = f_{\text{ph}} \left[ \frac{\lambda K(\lambda, t) - \lambda^{-2} K(\lambda^{-1}, t)}{\lambda - \lambda^{-2}} \right] \quad (11)$$

where the time dependence is introduced to the  $K$  function as

$$K(\lambda, t) = B(t) \left[ \frac{\dot{B}(t)}{B(t) + 1} + \kappa(t)^{-1} \frac{\lambda^2 \dot{B}(t) + B(t)}{B(t) + \kappa(t)\lambda^{-2}} \right] \quad (12)$$

with

$$B(t) = \kappa(t)^2 \frac{\lambda^2 - 1}{[\lambda^2 + \kappa(t)]^2} \quad (13)$$

$$\dot{B}(t) = B(t) \left[ \frac{1}{\lambda^2 - 1} - \frac{2}{\lambda^2 + \kappa(t)} \right] \quad (14)$$

The parameter  $\kappa(t)$  now becomes the only additional parameter to describe the relaxation behaviour of the networks.

### Dynamic constrained junction model for filled networks

In the dynamic constrained junction model, force acting on the network is given by equation (4) where,  $f_{\text{ph}}$  is the component of the force due to the phantom network, and  $f_{c,\text{eq}}$  and  $f_c(t)$  are the equilibrium and non-equilibrium forces due to the constraints respectively. For filled networks, the authors make the simplest assumption that all components of the force in equation (4) follow the Guth and Gold form<sup>18-21</sup>

$$f_{\text{ph}} = (f_{\text{ph}})_0 \left( 1 + 2.5\phi + 14.1\phi^2 \right) \quad (15)$$

$$f_{c,\text{eq}} = (f_{c,\text{eq}})_0 \left( 1 + 2.5\phi + 14.1\phi^2 \right) \quad (16)$$

$$f_c(t) = [f_c(t)]_0 \left( 1 + 2.5\phi + 14.1\phi^2 \right) \quad (17)$$

where subscript 0 describes the unfilled amorphous network,  $\phi$  is the effective volume fraction which includes the occluded rubber as mentioned in the introduction section. When equation (6) is rearranged by multiplying and dividing by  $f_{\text{ph}}$ , then the following can be obtained

$$f(t) = (f_{\text{ph}}) \left\{ 1 + \frac{(f_{c,\text{eq}})}{(f_{\text{ph}})} + \frac{[f_c(t)]}{(f_{\text{ph}})} \right\} \quad (18)$$

In this equation, the second and the third terms in the brackets are independent of  $\phi$  and only the third term is

time dependent. Additionally, only the first  $f_{\text{ph}}$  term of the right hand side of the equality is  $\phi$  dependent. In equations (16) and (17), it is implicitly assumed that the kappa parameter is unchanged by the presence of filler. Values of this parameter obtained from best fitting functions to experimental data, described below, show that there is a small dependence of  $\kappa_0$  in filled samples. The constancy of the  $\kappa$  parameter is the assumption of the model and has to be validated with further experiments. In the following, the authors keep the  $\kappa_0$  parameter as a fitting variable.

## Experimental

### Materials

The raw materials used in this recipe were Natural rubber (poly)isoprene, zinc oxide, stearic acid, CBS (N-cyclohexyl-2-benzothiazole sulphenamide), carbon black (N330) and sulphur. All the raw materials were used as received. The natural rubber grade was ribbed smoked sheet, RSS1, with a Mooney viscosity of 85 Mooney Units, MU, at 100°C, MW ≈ 350 000 and a polydispersity index of 2.5, supplied from Eversharp Rubber Industries, Jalan, Singkang, Jementah, Johor. Zinc oxide, 99.7% purity with a 550 g L<sup>-1</sup> bulk density was supplied from Metal Oksit (www.metaloksit.com). Stearic acid with an acid value 208.8 mg KOH g<sup>-1</sup>, fatty acid composition 55.2% C16, 44.2% C18 was supplied from Natoleo (www.natoleo.co.kr). Carbon black was supplied from TUPRAŞ (www.tupras.com.tr) with a DBP absorption of 102 mL per 100 g, with an iodine adsorption of 83.2 mg g<sup>-1</sup> and with a bulk density of 378 g L<sup>-1</sup>. CBS was supplied from MLPC. Its melting point was 97°C, ash content was 0.3% and specific gravity was 1.27. Sulphur was supplied from MLPC (www.mlpc-intl.com). Its melting point was 115°C and specific gravity was 2.04.

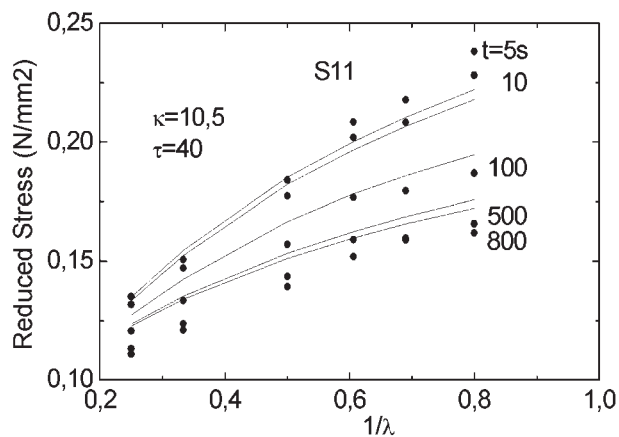
### Compounding

Compounds were prepared by using a lab scale 1.5 litre Werner & Pfleiderer internal mixer. This internal mixer has standard tangential rotor geometry. The homogenisations were made on the two roll open mills. Rubber was fed into the chamber, masticated for 2 min and then zinc oxide and stearic acid were added. The compound was dumped at ~135°C. It was homogenised on the two roll mill for 5 min. In the second stage, for the filled elastomers, carbon black was first incorporated and then accelerator and sulphur were added on the two roll mill for different compounds.

### Vulcanisation

Vulcanisation was carried out in a compression moulding with 160 t clamping force. All test sheets were vulcanised at 150°C for 35 min. The test sheet dimensions were 210 × 300 × 2 mm.

Before the test sheets were vulcanised, rheometer curves were checked at 150°C which is the temperature at which the test sheets were vulcanised later on. The rheometer curves showed that the torque values reach a plateau and remained constant from thereon, indicating that there is no reversion. The optimum cure times were obtained between 25 and 30 min depending on the different cross-linking densities in the rheometer curves. To be on the safe side, all sheets were vulcanised at



2 Isochronous plots of sample S11 and comparison with dynamic constrained junction model results

150°C for 35 min knowing that there is no reversion for these recipes.

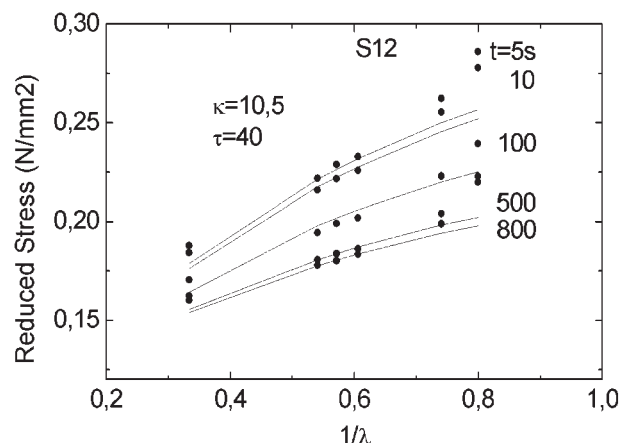
### Relaxation tests

Dumbbell shaped test specimens of 2 mm thickness were cut out from the vulcanised sheets with the help of a Zwick sample cutter in accordance with DIN 53 504, S1. Relaxation tests were carried out in a Zwick Roell Z2.5 universal tensile machine (UTM) with a load cell of 2.5 kN. Extension data were acquired at every 10 μm with an accuracy of 1%. The equipment used testXpert V10.1 version software. Dumbbell shaped test sheets were tested at UTM with a preload of 0.2 N that prevented the initial curvature of the free samples. Test sheets were stretched to different extension ratios at a speed of 800 mm min<sup>-1</sup>, and relaxed for 880 s. for every sample. Data were taken at every 0.02 s. during the test. In order to simplify presentation, the authors use the notation in Table 1 for sample designation.

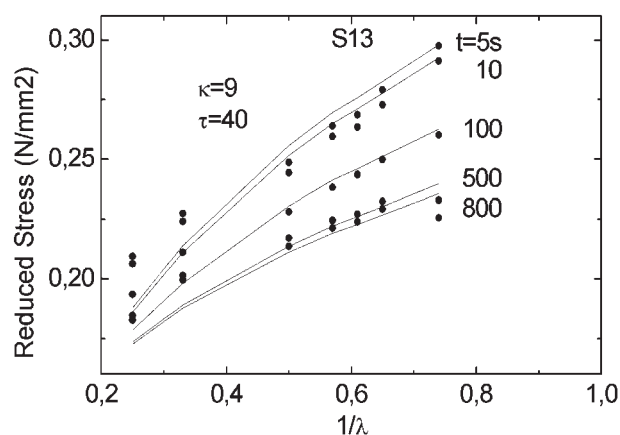
### Results

In order to reduce the size of the paper, the authors present results for only the samples S11, S12 and S13. Results for the other samples are similar, which may be obtained from the authors at the indicated addresses.

In Figs. 2–4, the authors present isochronous plots for networks with different filler amounts and cross-link densities. The ordinates denote the reduced stress [ $f^*$ ] and the abscissa are the reciprocal extension ratios. The points show the results of experiments. The shortest time



3 Isochronous plots of sample S12 and comparison with dynamic constrained junction model results



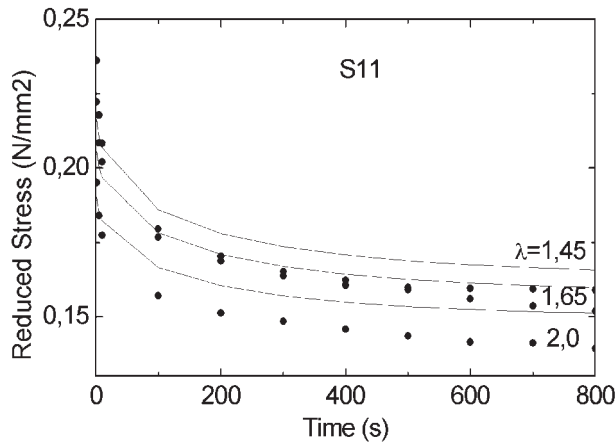
4 Isochronous plots of sample S13 and comparison with dynamic constrained junction model results

of observation is one second. The longest time of 880 s recorded in the experiments did not correspond to full equilibrium, but sufficiently close to it for all of the samples. The curves are obtained from the theory presented in reference<sup>11</sup> with the exception that  $f(t)$  is calculated by using equation (18) given in this paper. The fitting parameters of  $\tau$ ,  $\beta$ ,  $(f_{ph})_0$  were calculated for the unfilled samples of different cross-link densities given in reference<sup>11</sup> and used in this paper as they are. These parameters can be seen in Table 1 as well. The only fitting parameter in this study is the  $\kappa_0$  for the filled samples and presented on each graph.

Table 1 Sample notation

Sample notation	Effective filler volume fraction $\phi$	Sulphur amount, phr	$\kappa_{eq}$	$(f_{ph})_0^*$ , N mm <sup>-2</sup>
S01	0	0.75	9.0	0.092
S02	0	1.00	8.0	0.104
S03	0	1.25	6.0	0.132
S11	0.0397	0.75	10.5	0.092
S12	0.0397	1.00	10.5	0.104
S13	0.0397	1.25	9	0.132
S21	0.0799	0.75	5.5	0.092
S22	0.0799	1.00	10.5	0.104
S23	0.0799	1.25	3.5	0.132
S31	0.1129	0.75	9.5	0.092
S32	0.1129	1.00	11.0	0.104
S33	0.1129	1.25	8.0	0.132

\*Taken from reference;<sup>11</sup> the relaxation time  $\tau=40$  s and the stretched exponent  $\beta=0.4$  for all samples.



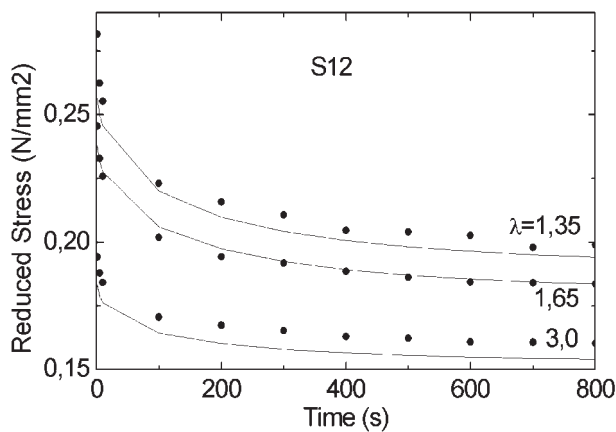
5 Dependence of stress on time for sample S11

In Figs. 5–7 the dependence of stress on time is presented for the three samples.

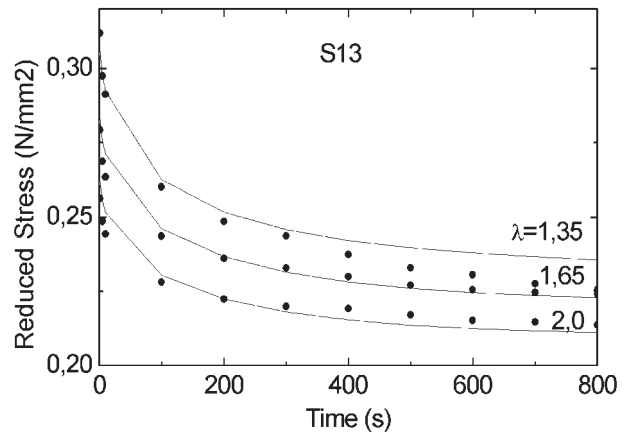
**Discussion**

In this study, the authors extended the dynamic constrained junction model to stress relaxation of filled samples of different cross-link densities in uniaxial tension. The basic assumption we made is that the phantom, equilibrium and non-equilibrium forces acting on the network obey the Guth and Gold equation dependence. The authors also used the occluded rubber for the effective volume of the fillers as proposed by Medalia. In the dynamic constrained junction model for unfilled networks there were four fitting parameters as given in reference<sup>11</sup> namely, phantom contribution ( $f_{ph}$ ), relaxation time,  $\tau$ , exponent,  $\beta$  and  $\kappa_0$ . Since the authors used the same cross-link densities in the present study with the reference,<sup>11</sup> the authors used three parameters out of four as they were found in the previous study. The authors only kept  $\kappa_{eq} = \kappa_0$  free as the fitting parameter in the present study. Values of  $\kappa_0$  obtained from curve fits are presented in Fig. 8 as a function of volume fraction of filler.

The solid straight line indicates the best linear fit. The dashed curves indicate the upper and lower 95% confidence limits. There is a small dependence of  $\kappa_0$  on filler content. However, in view of the large scatter in the ordinate values, it can be concluded that this dependence is insignificant.



6 Dependence of stress on time for sample S12

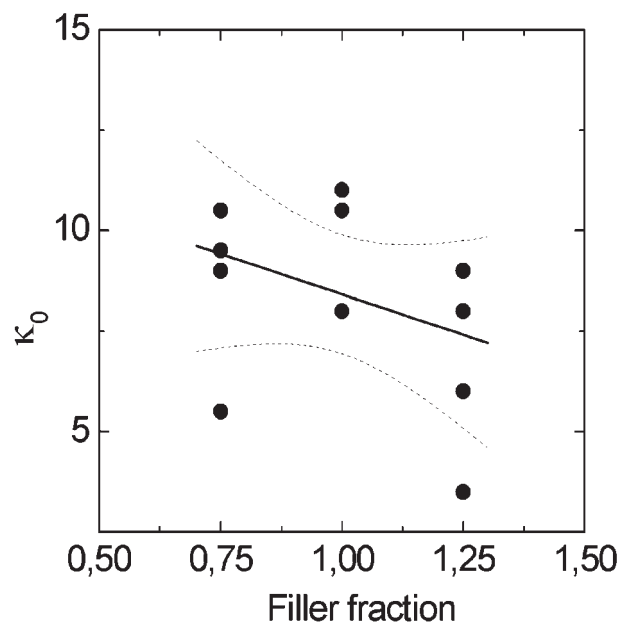


7 Dependence of stress on time for sample S13

The three major conclusions of the present model and experimental observation are the following:

- (i) assumption of Guth and Gold relations for the equilibrium and time dependent forces given by equations (15)–(17) are satisfactory
- (ii) for the same cross-link density, the same characteristic relaxation time describes the unfilled and filled samples
- (iii) considering that only one variable,  $\kappa_0$ , is adjustable, the deformation dependence of the stress is predicted satisfactorily for filled networks by the dynamic constrained junction model. The deviations of the reduced force between theory and experiment at large deformations are observed in general for unfilled networks as well. This deviation may be partly due to the finite chain extensibility effects, which are not considered in the theoretical model.

As stated in the introduction, higher filler amounts introduce new physics into the network problem, and therefore the simple molecular model of the present paper cannot be expected to hold at higher filler loadings.



8 Calculated values of  $\kappa_0$  as a function of volume fraction of filler

## References

1. J. E. Mark and B. Erman: 'Rubberlike elasticity, a molecular primer'; 1988, New York, John Wiley & Sons.
2. B. Erman and J. E. Mark: 'Structures and properties of rubberlike networks'; 1997, New York, Oxford University Press.
3. J. E. Mark and B. Erman: 'Rubberlike elasticity: a molecular primer'; 2007, New York, Cambridge University Press.
4. B. Erman and P. J. Flory: *Macromolecules*, 1982, **15**, 806–812.
5. P. J. Flory: *J. Phys. Chem.*, 1977, **66**, 5720–5729.
6. P. J. Flory and B. Erman: *Macromolecules*, 1982, **15**, 800–806.
7. B. Erman and J. E. Mark: 'Structures and properties of rubberlike networks'; 1997, New York, Oxford University Press.
8. B. Ewen and D. Richter: in 'Molecular basis of polymer networks', (ed. A. Baumgartner and C. E. Picot), Vol. 42, 82–92; 1989, Berlin, Springer-Verlag.
9. B. Ewen and D. Richter: *Adv. Polym. Sci.*, 1997, **134**, 1–129.
10. J. W. M. Noordermeer and J. D. Ferry: *J. Polym. Sci. Polym. Phys. Ed.*, 1976, **14**, 509–520.
11. H. Konyali, Y. Menciloglu and B. Erman: *Polymer*, 2008, **49**, 1056–1065.
12. A. Botti, W. W. Pyckhout-Hintzen, D. Richter, V. Urban and E. Straube: *J. Chem. Phys.*, 2006, **124**, 174908–174912.
13. J. S. Bergstrom and M. C. Boyce: *Mech. Mater.*, 2000, **32**, 627–644.
14. A. D. Drozdov and A. Dorfmann: *Int. J. Solids Struct.*, 2002, **39**, 5699–5717.
15. A. Lion: *Continuum Mech. Thermodyn.*, 1996, **8**, 153–169.
16. A. D. Drozdov and A. Dorfmann: *Int. J. Plastic.*, 2003, **19**, 1037–1067.
17. H. B. Callen: 'Thermodynamics and an Introduction to thermo-statistics'; 1985, New York, Wiley.
18. H. M. Smallwood: *J. Appl. Phys.*, 1944, **15**, 758–766.
19. E. Guth and O. Gold: *Phys. Rev.*, 1938, **53**, 322–328.
20. G. Heinrich, M. Kluppel and T. A. Vilgis: *Curr. Opin. Solid State Mater. Sci.*, 2002, **6**, 195–203.
21. E. Guth: *J. Appl. Phys.*, 1945, **16**, 20–25.